Published in final edited form as:
J Mol Cell Cardiol. 2008 January ; 44(1): 47–58. doi:10.1016/j.yjmcc.2007.06.008.

PRDM6 is enriched in vascular precursors during development and inhibits endothelial cell proliferation, survival, and differentiation

Yaxu Wu[*], **James E. Ferguson III**[*], **Hong Wang**[*], **Rusty Kelley**[*], **Rongqin Ren**[*], **Holly McDonough**[*], **James Meeker**[*], **Peter C. Charles**[*], **Hengbin Wang**[#], and **Cam Patterson**[*,†]

* *Carolina Cardiovascular Biology Center, University of North Carolina, Chapel Hill, NC*

† *Departments of Medicine, †Cell and Developmental Biology, and †Pharmacology, University of North Carolina, Chapel Hill, NC*

Department of Biochemistry and Molecular Genetics, University of Alabama at Birmingham

Abstract

The mechanisms that regulate the differentiation program of multipotential stem cells remain poorly understood. In order to define the cues that delineate endothelial commitment from precursors, we screened for candidate regulatory genes in differentiating mouse embryoid bodies. We found that the PR/SET domain protein, PRDM6, is enriched in flk1(+) hematovascular precursor cells using a microarray-based approach. As determined by 5′ RACE, full length PRDM6 protein contains a PR domain and four Krüpple-like zinc fingers. In situ hybridization in mouse embryos demonstrates staining of the primitive streak, allantois, heart, outflow tract, para-aortic splanchnopleura (P-Sp)/aorto-gonadal-mesonephric (AGM) region and yolk sac, all sites known to be enriched in vascular precursor cells. PRDM6 is also detected in embryonic and adult-derived endothelial cell lines. PRDM6 is co-localized with histone H4 and methylates H4-K20 (but not H3) in vitro and in vivo, which is consistent with the known participation of PR domains in histone methyltransferase activity. Overexpression of PRDM6 in mouse embryonic endothelial cells induces apoptosis by activating caspase-3 and inducing G1 arrest. PRDM6 inhibits cell proliferation as determined by BrdU incorporation in endothelial cells, but not in rat aortic smooth muscle cells. Overexpression of PRDM6 also results in reduced tube formation in cultured endothelial cells grown in Matrigel. Taken together, our data indicate that PRDM6 is expressed by vascular precursors, has differential effects in endothelial cells and smooth muscle cells, and may play a role in vascular precursor differentiation and survival by modulating local chromatin-remodeling activity within hematovascular subpopulations during development.

Keywords

endothelium; stem cell; PR domain; proliferation

Address correspondence and inquiries to: Cam Patterson, M.D., Director, Division of Cardiology and Carolina Cardiovascular Biology, University of North Carolina at Chapel Hill, 8200 Medical Biomolecular Research Building, Chapel Hill, NC 27599-7126, Tel.: (919) 843-6477, Fax: (919) 966-1743, e-mail: E-mail: cpatters@med.unc.edu.

INTRODUCTION

The early development of endothelial and hematopoietic lineages is closely related spatiotemporally in the vertebrate embryo and may involve a common precursor, the hemangioblast. Persistent expression of flk1 in these cells is associated with differentiation along the endothelial cell lineage, whereas loss of flk1 expression characterizes differentiating progeny [1]. Targeted disruption of the flk1 gene in mice leads to absence of both endothelial and hematopoietic development and death *in utero* at E8.0-E9.0, indicating a requirement for flk1 in the earliest stages of hematovascular development [2]. Embryonic stem (ES) cell-derived embryoid bodies have been used to track hemangioblast induction and specification to the endothelial or hematopoietic lineage, and flk1 (+) cells define a major population of hemangioblasts [3,4]. Vascular cells derived from flk1 (+) cells can organize into vessel-like structures consisting of endothelial tubes supported by mural cells in three-dimensional culture, demonstrating that flk1 is not only one of most specific markers highlighting the earliest stage of hematopoietic and vascular lineages, but that flk1+ precursors may also contribute to mural lineages and cardiomyocytes, acting as 'vascular progenitor cells' [5,6].

We have sought to identify molecular determinants of vascular formation using an *in vitro* ES cell differentiation system by analyzing global expression patterns in the developing vasculature. This approach, for example, has revealed the importance of Wnt activation during differentiation of flk1+ precursors [7]. In the course of this analysis, we also noted the preferential expression of PRDM6, a PR/SET domain containing protein, in flk1+ cells at selected time points during differentiation. The PR domain, first noted as the *PRDI-BF1-RIZ1* homologous region, characterizes a subfamily of Krüppel-like zinc finger genes that function in cell-fate decision and malignant transformation [8–13]. A splice variant of PRDM6 was recently identified in a search for mRNAs highly expressed in aortic smooth muscle [14]. It was characterized as an SMC-restricted epigenetic regulator, and therefore named PRISM/PRDM6 (*PR domain in smooth muscle*). Here we report the cloning and characterization of multiple full-length isoforms of PRDM6, characterize its expression in sites known to be enriched in vascular precursor cells during embryogenesis, and demonstrate its gene functions in endothelial cells, including methylation of histone H4 (but not H3), induction of apoptosis and cell-cycle arrest at G1, and reducing tube formation in endothelial cells. These results suggest roles for PRDM6 in early stages of vascular precursor differentiation and survival by modulating local chromatin-remodeling activity within hematovascular subpopulations during development.

MATERIALS AND METHODS

Cell lines

Mouse myocardial endothelial cells (MEC), Py-4-1 mouse hemangioma endothelial cells, C166 mouse embryonic yolk sac endothelial cells, mouse aortic smooth muscle cells (MASM) and rat smooth muscle cells (RASM) were grown in DMEM with 10% FBS [15]. Neonatal rat cardiomyocytes (RCM) were isolated as previously described [16].

5′ RACE

The 5′ region of mouse PRDM6 cDNA was cloned by rapid amplification of cDNA ends using total RNA from sorted flk1 (+) cell populations of differentiated ES cells. The primer used for 5′ RACE was: *5′*—CTTTTGTTGAAGGGCTGCAGGGCAT—3′.

Construction of PRDM6 expression plasmids

5′ ready cDNA was used as a template for amplification of full-length PRDM6 cDNA. Sequence containing the putative initiation codon from 5′ RACE product was used as the 5′

primer and the sequence containing the putative stop codon was used as the 3′ primer. The PCR products were cloned and sequenced. Four novel isoforms of PRDM6 were generated. For mammalian expression, the coding sequence were cloned into pCMVtag2B to create pPRDM6/4#, pPRDM6/3#, pPRDM6/33# and pPRDM6/36#, with an amino-terminal FLAG tag for immunodetection.

Northern blot analysis, in situ hybridization and RT-PCR

Northern blot analysis was conducted as described with a DNA probe from 210 bp to 594 bp of PRDM6/4# (a fragment common to all isoforms) [17]. For *in situ* hybridization, embryos were collected at different times from pregnant CD-1 mice. After fixation in 4% paraformaldehyde, embryos were stained with a digoxigenin-labeled antisense RNA probe (from 165 bp to 1132 bp) or a respective sense control. Digoxigenin was detected with an alkaline phosphatase-conjugated antibody, and the reaction was developed by adding nitroblue tetrazolium. The oligonucleotides used for RT-PCR to detect specific gene expression were: mouse PRDM6 (sense: 5′—CGTAATGGAAGCCATGTGCCGACAG—3′, antisense: 5′—CAGGAGAATGCGCTGCGTGAAAGTC—3′); and GAPDH (sense: 5′—ACCACAGTCCATGCCATCAC—3′; antisense: 5′—TCCACCACCCTGTTGCTGTA—3′).

Confocal immunostaining assay

Immunostaining of cultured cells with anti-FLAG, anti-Histone H4 antibody (Abcam) and DAPI was performed as previous described [15]. Confocal immunostaining images were collected using a Leica SP2-AOBS confocal microscope and analyzed with Leica Confocal Software.

Histone methyltransferase (HMTase) assay

HMTase assays were performed essentially as described [18]. Briefly, similar amounts of proteins were immunoprecipitated from transfected HEK293 cells with Anti-FLAG-M2 affinity gel, and then were incubated with core histones (4 μg) in 32.5 μl reactions containing 20 mM Tris-HCl (pH 8.0), 4 mM EDTA, 1 mM PMSF, 0.5 mM DTT, and 1 μl ^{3}H-SAM (15 Ci/mM; NEN Life Science Products) for 1 hr at 30°C. Proteins were separated in an 18% SDS-PAGE. For methylation site determination, HeLa cells were used for transfection and HMT assays were carried out with 2 mM of unlabeled SAM. Methylation sites were detected by Western blot analysis with specific antibodies. GST-SET7 was used as a control for H3-K4 methylation. For *in vivo* HMTase assays, core histones were purified from transfected HeLa cells and were then probed with specific antibodies as indicated.

Recombinant adenovirus and infection assays

PRDM6-expressing recombinant adenovirus was constructed by inserting Flag-tagged PRDM6/4# gene into GFP-expressing AdTrack. Cells seeded at 2×10^6 cells per 10-cm plate were incubated with adenovirus for 1 h in serum-free media. The media were then supplemented with serum to 10% and the culture was continued for the indicated times.

Growth, cell cycle and apoptosis assays

Living cell numbers were counted by trypan blue exclusion after 24 h of infection. Infected cells were also collected 18 h post infection and processed for DNA histogram analysis [19]. Cells were dispersed with trypsin/EDTA and were pooled with cells in the culture medium [20]. These cells were washed once with cold PBS and fixed with 80% ethanol. Cells were then washed once in PBS/0.2% BSA and incubated in propidium iodide/RNase A for 30 min. The stained cells were analyzed using a Becton Dickinson FACScan with Cytomation Summit software.

BrdU cell proliferation assay

Cell proliferation assessment using BrdU incorporation was carried out using a modified technique [21]. Briefly, cells infected for 18 h were pulse-labeled for 1 h with 10 μM BrdU. Cells were fixed and permeabilized with 2M HCl followed by subsequent washes with 0.1 M sodium tetraborate and PBS. BrdU incorporation was demonstrated by incubation with a PE-conjugated anti-BrdU mAb in buffer (10 mM HEPES, 150 mM NaCl, 0.04% FBS, 0.1% NaAz, 0.5% Tween 20) for 30 min, washed twice with the same buffer and then stained with 7-AAD. The stained cells were analyzed using a Becton Dickinson FACScan with Cytomation Summit software. The samples were analyzed for two-parameter dot plot histogram analysis (BrdU incorporation vs. DNA content) [22].

Tube formation assay

48-well plates were coated with growth factor-reduced Matrigel (Becton Dickinson) at 4°C and incubated for 30 minutes at 37°C. MEC or C166 cells were infected with AdPRDM6 or AdGFP for 9 h and then were trypsinized and seeded into Matrigel-coated wells at a density of 5×10^4 cells. After 12 h incubation, cells were observed under bright light and fluorescence microscope. Total tube length per field was measured and analyzed using Image J software [23,24].

RESULTS

Preferential expression of PRDM6 gene in flk1(+) vascular precursor cells

Using an unbiased microarray assay of *in vitro* differentiated ES cells, we have identified genes potentially involved in the earliest stages of endothelial cell differentiation in flk1(+) populations [7]. Approximately 22000 mRNAs were analyzed, and we identified a sequence for PRDM6 among the most differentially expressed genes (Figure 1*A*). We found PRDM6 was preferentially expressed in flk1 (+) cells at early stages of differentiation, with the highest enrichment of 8-fold at 84 hr (Figure 1*B*). RT-PCR confirmed strong preferential expression of this cDNA in flk1 (+) cells derived from embryoid bodies (Figure 1*C*). Remarkably, this differential expression is lost after 8 days of differentiation, when flk1 (+) cells are primarily mature endothelia.

Characterization of the PRDM6 gene

To characterize the potential function of PRDM6 during vascular development, we cloned the gene through 5′ RACE using an internal primer. An initial 1.5 kb fragment of PRDM6 contains a single open reading frame and the nucleotide sequence around the first methionine conforms to the Kozak initiator sequence GACATG [25]. We were able to isolate the full-length mouse PRDM6 cDNA using primer sequences covering the putative initiation codon and stop codon to generate a 565 a.a species of PRDM6 (which we designated PRDM6/4#) in which the amino-terminal 170 amino acids are unique, and the remainder of the protein is identical with PRISM/PRDM6 (Figures 2*A* and 2*B*) [14]. Analysis of the predicted protein by comparison with the SMART algorithm (http://smart.embl-heidelberg.de) indicated the presence of a PR domain and four zinc finger motifs at the carboxyl terminus (Figure 2*A*). These domains are all characteristic of PR family proteins.

The gene is located on mouse chromosome 18 and contains 8 exons spanning 110.5 kb (See Supplemental Figure). Further screening of PCR products and sequence analysis revealed three more isoforms of PRDM6, referred to herein as PRDM6/3#, 33#, and 36# (Figure 2*C*). Sequence alignment among the isoforms and comparison with the genomic sequence revealed that insertions near the amino terminus were generated by alternative splicing. The additional sequences of 31 residues in both PRDM6/3# and PRDM6/33# retain the first intron that is

spliced from PRDM6/4#. Similarly, PRDM6/36# has alternative splicing 3 base pairs upstream of the intron1/exon2 boundary, resulting in a single amino-acid insertion compared to PRDM6/4#. PRDM6/33# also has an internal alternative splicing event that results in the deletion of exons 3–5 of PRDM6/4# to become a PR-minus isoform. A unique carboxyl-terminal sequence is also found in PRDM6/36# from a single novel exon 8 that results from alternative splicing in intron 7 of PRDM6/4#. Since exon 8 of PRDM6/36# includes an in-frame stop codon, it encodes 48 residues of a unique carboxyl terminus lacking a fourth zinc finger. Generation of multiple isoforms from a single gene is typical of PR domain-containing proteins [26–28].

Expression patterns of PRDM6

The embryonic and adult tissue expression of PRDM6 in mice was determined by Northern blot analysis. PRDM6 is detectable as early as E7.5 with expression in the allantois, yolk sac, and placenta (Figure 3*A*). In adult mice, mRNA expression was highest in the spleen, lung, ovary and bone marrow, and lower levels of expression were detected in the heart (Figure 3*B*). Murine PRDM6 mRNA was expressed as a major band around 4 kb in embryos and tissues, with two shorter and one longer form of mRNA indicating alternative PRDM6 transcripts. Analysis of cell lines by RT-PCR revealed PRDM6 mRNA in MASM, RCM, cell lines derived from yolk sac (C166) and intraembryonic myocardial endothelial cells (MEC). The anatomical distribution of PRDM6 mRNA during embryogenesis was mapped by *in situ* hybridization with staining first detected in allantois/primitive streak regions at E7.5 (Figure 3*D*). Analysis of mouse embryos at E8.5–E9.5 showed characteristic staining in the heart and P-Sp/AGM region that hosts hematovascular progenitors (Figures 3*E* and 3*G*), and persistent staining of the allantois. Additionally, expression in the outflow track and yolk sac vasculature was evident at E9.5 (Figures 3*H* and 3*I*). Hybridization with sense mRNA demonstrated the specificity of this expression pattern (Figure 3*F*). Taken together, these data indicate that PRDM6 is expressed in sites enriched for vascular precursor cells in both the embryonic and the extraembryonic compartments.

Identification of PRDM6 as an H4-k20 Specific HMTase

To examine PRDM6 function, PRDM6 isoforms were subcloned into a mammalian expression vector and transiently transfected into HEK293 cells to generate FLAG-tagged fusion proteins that were detectable as an appropriately sized protein by Western blot analysis (*data not shown*). PRDM6/4# was located in the nucleus as determined by immunofluorescence analysis (Figure 4*A*). PRDM6/33# and PRDM6/36# isoforms were also localized to the nucleus, and PRDM6/36# was expressed in what appeared to be the nuclear envelope region (data not shown). Confocal microscopic colocalization studies revealed the overlapping expression of PRDM6/4# with histone H4 within the nucleus (Figure 4*B*). Based on the presence of the PR domain, we hypothesized that PRDM6 might be able to transfer methyl groups onto suitable substrate proteins. PRDM6 isoforms were immunopurified from HEK293 cell extracts and analyzed using an *in vitro* histone methyltransferase assay with core histones as the substrate. SET7, a highly active H3-K4 specific HMTase, was used as a positive control. The immunoprecipitated PRDM6/4# protein had methyltransferase activity selective to histone H4 and not to other histones, although the activity was weak (Figure 4*C*, top panel). PRDM6/33# and PRDM6/36#, to our surprise, also specifically methylated H4. PRDM6/33#, which lacks a PR domain, showed stronger HMTase activity when equal amounts of enzymes (Figure 4*C*, lower panel) were applied to equal amounts of core histones (Figure 4*C*, middle panel). The fact that PRDM6/33# retains histone H4 methyltransferase activity suggests that PRDM6 contains histone H4 methyltransferase activity independent of the PR domain or that PRDM6 interacts with other HMTase proteins. Because recombinant PRDM6 proteins purified from bacteria lack HMTase activity in this assay (*data not shown*), it seems most likely that PRDM6 associates with another protein in mammalian cells that is required for HMTase activity. This

would be analogous to the situation with PRDM1/PRDI-BF1/Blimp-1, another PR domain-containing protein that also requires a co-purifying partner protein for activity [29].

To further identify the target amino acid residue of PRDM6, FLAG-tagged PRDM6/4# and SET7 were recovered from transfected HeLa cells, and *in vitro* HMTase assays were carried out. As expected, both GST-SET7 and SET7 methylated H3-K4 (data not shown), whereas PRDM6 selectively methylated H4 at lysine20 (Figure 4*D*). We also examined whether PRDM6 has methyltransferase activity towards H4-K20 *in vivo*. To this end, Flag-tagged PRDM6/4# and SET7 were transfected into HeLa cells respectively. Core histones purified from the transfected cells were analyzed by Coomassie blue staining and Western blotting using antibodies specific for methylated H4-K20 [30]. As seen in Figure 4*E*, overexpression of PRDM6 had an obvious effect on H4-K20 methylation, which indicates that PRDM6 methylates H4-K20 *in vivo*. Collectively, these data suggest that PRDM6 is responsible for H4-K20 methylation *in vitro* and *in vivo*. Notably, this conclusion differs from previous suggestions that PRISM/PRDM6 is a histone H3 methyltransferase [14].

Detection of apoptosis and cell cycle arrest caused by PRDM6 in MEC

Our attempts to knock down PRDM6 expression via siRNA technology were hampered because of alternative splicing within the PRDM6 gene, leading to upregulation of various alternative isoforms when specific exons were targeted. Therefore, recombinant adenovirus AdPRDM6 was made with FLAG-PRDM6/4# and infected into MEC to determine the cellular effects of PRDM6 in cultured endothelial cells. AdPRDM6-infected cells grew more slowly than cells infected with control AdGFP, and cell death (as determined by Trypan blue inclusion) became apparent 24 h post infection in 40% of cells, whereas control virus-infected cells did not exhibit significant cell death (Figure 5*A*). To characterize the cell death caused by overexpression of PRDM6, infected cells were harvested at different time points. PRDM6 protein expression was evident at 9 h post infection and activation of apoptotic marker caspase-3 was first detected at 15 h, indicating activation of the caspase-3 terminal apoptotic pathway in PRDM6-induced apoptosis (Figure 5*B*). DNA content analysis with PI staining was performed as an independent assay for apoptosis. Decreased cell size and increased refractory index were observed in AdPRDM6 infected cells, a feature of apoptotic cells. Quantitation of percentages of cells within different phases of the cell cycle demonstrated a significant increase of apoptotic cells and cell cycle arrest at G_1 in PRDM6-infected endothelial cells (Figure 5*C*). In contrast, AdFGP-infected cells were mostly in G_1 and did not undergo apoptosis. These experiments indicate that PRDM6 can induce G_1 arrest and/or apoptosis in MEC (Figure 5*D*).

Effect of PRDM6 overexpression on cell proliferation is cell-type dependent

These observations were surprising insofar as overexpression of PRISM/PRDM6 has previously been shown to elicit a modest proliferative response in smooth muscle cells by inhibiting genes associated with the differentiation pathway [14]. This discrepancy prompted us to characterize PRDM6-induced cell-cycle arrest in more detail. DNA synthesis rate was evaluated by incorporation of BrdU into DNA by flow cytometry. As shown in Figure 6*A*, endothelial cells overexpressing PRDM6 had a lower ratio of BrdU incorporation (25 %) compared with AdGFP-infected cells (40 %). To confirm that over-expression of PRDM6 has different effects in two different cell lines, BrdU incorporation assay was conducted with RASM with the same conditions. In contrast with endothelial cells, there was no suppression of BrdU uptake in smooth muscle cells (Fig 6*B*). The BrdU incorporation results are summarized in (Fig 6*C*). These results indicate that PRDM6 has differential effects on viability and proliferation among cells within the vascular lineage. This may explain the loss of preferential expression of PRDM6 we observed at times when endothelial cells have matured (Figure 1*C*).

Effects of PRDM6 on endothelial cell assembly in vitro

To further explore the effects of PRDM6 on endothelial function, we utilized a Matrigel-based culture system that provides a method to evaluate key components in neovascular growth: directional endothelial cell migration, cell-cell contact and pattern formation. The effects of PRDM6 in this system were examined in two embryonic endothelial cell lines, MEC and C166, using growth factor-reduced Matrigel. When infected with AdGFP, both cell lines migrated, attached to one another and formed microvessel-like structures on reconstituted basement membrane that resemble a remodeling capillary bed (Figures 7*A* and 7*B*). In contrast, AdPRDM6-infected cells had markedly diminished capacity to assemble organized structures (summarized in Figure 7*C*), with markedly limited numbers of cells remaining alive, underscoring an antagonistic role of PRDM6 on events that are required for normal endothelial cell survival and differentiation in vascular structures.

DISCUSSION

In this report we have shown that PRDM6 is preferentially expressed in fk1(+) cells in differentiated ES cells and in the allantois, primitive streak, P-Sp/AGM regions and yolk sac during mouse development (Figures 3), all regions known to host vascular precursors [31–37]. In agreement with previous data, PRDM6 is expressed in adult aortic SMC and is also detected in embryo-derived endothelial cells (Figure 3) [14]. This pattern of expression pattern suggests a role for PRDM6 in early stages of vascular development, and provided us with an impetus to characterize the function of this protein further.

The presence of the PR/SET domain raised the strong possibility that PRDM6 may have HMTase activity, although this activity is not intrinsic to all PR-domain containing proteins. For example, PRDM2/RIZ methylates histone H3 on lysine 9 through an intrinsic activity that requires the PR domain [38]. In contrast, PRDM1/PRDI-BF1/Blimp-1, another PR domain protein, participates in methyltransferase reactions although its HMTase activity is extrinsic, exerting HMTase activity in transcriptional silencing only when G9a, a Histone H3-K9 and K27 dimethyl HMTase, is recruited into a complex [29,39]. Interestingly, PRISM/PRDM6 was also reported to associate with G9a and methylate Histone H3 [14]. In this report, we demonstrate in contrast that immunopurified full-length PRDM6 isoforms are able to methylate histone H4-K20 (but not other histones) in a PR domain-independent fashion (Figure 4*C*). It is not clear if additional amino-terminal sequences or co-associating proteins confer this function at the present time. Defining the functional domains or interacting partners of PRDM6 responsible for its HMTase activity will be an important area of future investigation.

All presently reported members of PR family proteins have growth repressive activity. For example, overexpression of PRDM2/RIZ1 and PRDM5 induces G_2/M cell cycle arrest and apoptosis in cancer lines [40,41]. Blimp-1 inhibits cell differentiation and induces apoptosis in a cell type-dependent fashion [42]. Similarly, we found that PRDM6 induces apoptosis and cell cycle arrested at G1 in endothelial cells, but not in smooth muscle cells (Figures 5 and 6). Based on our determination that PRDM6 is preferentially expressed in flk1(+) vascular precursor cells and its differential effects on endothelial and smooth muscle cells, we speculate that PRDM6 may coordinate cell fate decisions in vascular progenitor cells that favor smooth muscle over endothelial differentiation, or may selectively ablate cells progressing down the endothelial lineage during early stages of vascular remodeling. This is consistent with the observation of Davis et al. that PRDM6 is expressed primarily in smooth muscle compartments at later stages of murine development [14].

To date, the best-characterized PR protein in cell fate choice is Blimp-1. In the B lymphocyte lineage, expression of this transcriptional repressor is restricted to mature B cell subsets, and early B cell development is unimpaired by Blimp-1 disruption [43]. Blimp-1 represses a series

of genes whose transcription factor products regulate growth control, apoptosis, antigen receptor signaling, and lineage commitment [44,45]. It was therefore widely accepted as a master regulator of plasma cell differentiation. Recently, two groups took different approaches to extend the function of Blimp1 to the homeostasis and activation in T cells [12,13]. The idea that Blimp-1 may function in early T cell maturation is suggested by the observation that double-positive thymocytes are reduced in number and are prone to apoptosis in mice with T cell–restricted Blimp-1 deletion [13]. It is likely that similar epigenetic mechanisms of regulation exist within the vascular developmental program, and our data indicate that PRDM6 is a likely candidate to participate in these regulatory programs that determine vascular cell fate.

Our data support the conclusions of Davis et al. that PRDM6 is a vascular-restricted protein that functions as an HMTase, although it is important to reconcile key differences between these studies [14]. The multiple sequences of PRDM6 that we identified have a long open reading frame with conserved Kozak sequences around the initiation codon, and conform to expressed sequence tags that are present in GenBank. The isoform PRDM6/4# is identical to PRISM/PRDM6, except that it has an additional amino-terminal 170 residues. PRISM/PRDM6 appears to represent an isoform expressed via an alternative promoter specifically in smooth muscle cells. Our data and those of Davis et al. support a role for PRDM6 in HMTase activity, but our data indicate that PRDM6 methylates histone H4 at lysine 20, whereas the previous report suggests that PRDM6 utilizes histone H3 as a substrate. A key difference between these reports is that Davis et al. used purified histone H3 alone in their assays, whereas we use a histone preparation that contains all nuclear histones in a natural stoichiometry. Thus, when all histones are present, histone H4 is clearly preferred as a PRDM6 substrate and no histone H3 methylation is detectible (even though we see histone H3 methylation by SET7 under the conditions of our experiments). Finally, we believe that the differential effects of PRDM6 on smooth muscle proliferation compared to the anti-proliferative and pro-apoptotic effects of PRDM6 we observe in endothelial cells (Figures 5 and 6) most likely represent biologically meaningful distinctions that may allow PRDM6 to determine cell fate decisions within vascular progenitor populations, a hypothesis that is strongly supported by the patterns of expression of PRDM6 in early and later stages of vascular development examined in our respective studies [14].

The PRDM gene family of transcriptional factors is characterized by the presence of multiple isoforms. Aside from the PR-plus and PR-minus variants, there are multiple other isoforms that can be generated by alternative splicing or by alternative promoter usage. Many lines of investigation suggest that PRDM genes seem to have a dual function that follows a similar pattern: the PR-plus isoform behaves as tumor suppressor, while the PR-minus isoform functions as an oncogene since the PR-plus product is found disrupted or underexpressed whereas the PR-minus product is present or overexpressed in many types of cancer cells [20–28]. Here we reported the discovery of four more isoforms of PRDM6 in addition to the reported PRISM/PRDM6 [14]. Isoforms PRDM6/4# and PRISM/PRDM6 apparently have different functions in the differentiation and proliferation of endothelial cells and smooth muscle cells respectively. It will be interesting to analyze the expression of gene variants in both cell types and in *in vitro* ES differentiation system. The proper balance of the variants, a result of either genetic or epigenetic events, might be critical in maintaining the chromatin-mediated control of gene expression and normal cell homeostasis during embryonic development.

Supplementary Material

Refer to Web version on PubMed Central for supplementary material.

Acknowledgements

We thank Dr. Dazi Wang for technical advices. C.P. is an Established Investigator of the American Heart Association and a Burroughs Wellcome Fund Clinician Scientist in Translational Research. This work was supported by grants HL 61656, HL 03658 and HL 072347 to C.P.

References

1. Yamaguchi TP, Dumont DJ, Conlon RA, Breitman ML, Rossant J. flk-1, an flt-related receptor tyrosine kinase is an early marker for endothelial cell precursors. Development 1993 Jun;118(2):489–98. [PubMed: 8223275]
2. Shalaby F, Rossant J, Yamaguchi TP, Gertsenstein M, Wu XF, Breitman ML, et al. Failure of blood-island formation and vasculogenesis in Flk-1-deficient mice. Nature 1995 Jul 6;376(6535):62–6. [PubMed: 7596435]
3. Choi K, Kennedy M, Kazarov A, Papadimitriou JC, Keller G. A common precursor for hematopoietic and endothelial cells. Development 1998 Feb;125(4):725–32. [PubMed: 9435292]
4. Fehling HJ, Lacaud G, Kubo A, Kennedy M, Robertson S, Keller G, et al. Tracking mesoderm induction and its specification to the hemangioblast during embryonic stem cell differentiation. Development 2003 Sep;130(17):4217–27. [PubMed: 12874139]
5. Yamashita J, Itoh H, Hirashima M, Ogawa M, Nishikawa S, Yurugi T, et al. Flk1-positive cells derived from embryonic stem cells serve as vascular progenitors. Nature 2000 Nov 2;408(6808):92–6. [PubMed: 11081514]
6. Kattman SJ, Huber TL, Keller GM. Multipotent flk-1(+) cardiovascular progenitor cells give rise to the cardiomyocyte, endothelial, and vascular smooth muscle lineages. Dev Cell 2006 Nov;11(5):723–32. [PubMed: 17084363]
7. Wang H, Charles PC, Wu Y, Ren R, Pi X, Moser M, et al. Gene expression profile signatures indicate a role for Wnt signaling in endothelial commitment from embryonic stem cells. Circ Res 2006 May 26;98(10):1331–9. [PubMed: 16601226]
8. Huang S. Blimp-1 is the murine homolog of the human transcriptional repressor PRDI-BF1. Cell 1994 Jul 15;78(1):9. [PubMed: 8033216]
9. Turner CA Jr, Mack DH, Davis MM. Blimp-1, a novel zinc finger-containing protein that can drive the maturation of B lymphocytes into immunoglobulin-secreting cells. Cell 1994 Apr 22;77(2):297–306. [PubMed: 8168136]
10. Buyse IM, Shao G, Huang S. The retinoblastoma protein binds to RIZ, a zinc-finger protein that shares an epitope with the adenovirus E1A protein. Proc Natl Acad Sci U S A 1995 May 9;92(10):4467–71. [PubMed: 7538672]
11. Fears S, Mathieu C, Zeleznik-Le N, Huang S, Rowley JD, Nucifora G. Intergenic splicing of MDS1 and EVI1 occurs in normal tissues as well as in myeloid leukemia and produces a new member of the PR domain family. Proc Natl Acad Sci U S A 1996 Feb 20;93(4):1642–7. [PubMed: 8643684]
12. Kallies A, Hawkins ED, Belz GT, Metcalf D, Hommel M, Corcoran LM, et al. Transcriptional repressor Blimp-1 is essential for T cell homeostasis and self-tolerance. Nat Immunol 2006 May;7(5):466–74. [PubMed: 16565720]
13. Martins GA, Cimmino L, Shapiro-Shelef M, Szabolcs M, Herron A, Magnusdottir E, et al. Transcriptional repressor Blimp-1 regulates T cell homeostasis and function. Nat Immunol 2006 May;7(5):457–65. [PubMed: 16565721]
14. Davis CA, Haberland M, Arnold MA, Sutherland LB, McDonald OG, Richardson JA, et al. PRISM/PRDM6, a transcriptional repressor that promotes the proliferative gene program in smooth muscle cells. Mol Cell Biol 2006 Apr;26(7):2626–36. [PubMed: 16537907]
15. Wu Y, Moser M, Bautch VL, Patterson C. HoxB5 is an upstream transcriptional switch for differentiation of the vascular endothelium from precursor cells. Mol Cell Biol 2003 Aug;23(16):5680–91. [PubMed: 12897140]
16. Li HH, Kedar V, Zhang C, McDonough H, Arya R, Wang DZ, et al. Atrogin-1/muscle atrophy F-box inhibits calcineurin-dependent cardiac hypertrophy by participating in an SCF ubiquitin ligase complex. J Clin Invest 2004 Oct;114(8):1058–71. [PubMed: 15489953]

17. Moser M, Binder O, Wu Y, Aitsebaomo J, Ren R, Bode C, et al. BMPER, a novel endothelial cell precursor-derived protein, antagonizes bone morphogenetic protein signaling and endothelial cell differentiation. Mol Cell Biol 2003 Aug;23(16):5664–79. [PubMed: 12897139]
18. Wang H, Cao R, Xia L, Erdjument-Bromage H, Borchers C, Tempst P, et al. Purification and functional characterization of a histone H3-lysine 4-specific methyltransferase. Mol Cell 2001 Dec; 8(6):1207–17. [PubMed: 11779497]
19. Gu JJ, Santiago L, Mitchell BS. Synergy between imatinib and mycophenolic acid in inducing apoptosis in cell lines expressing Bcr-Abl. Blood 2005 Apr 15;105(8):3270–7. [PubMed: 15604220]
20. Jiang G, Liu L, Buyse IM, Simon D, Huang S. Decreased RIZ1 expression but not RIZ2 in hepatoma and suppression of hepatoma tumorigenicity by RIZ1. Int J Cancer 1999 Nov 12;83(4):541–6. [PubMed: 10508492]
21. Aarbiou J, Ertmann M, van Wetering S, van Noort P, Rook D, Rabe KF, et al. Human neutrophil defensins induce lung epithelial cell proliferation in vitro. J Leukoc Biol 2002 Jul;72(1):167–74. [PubMed: 12101277]
22. Mauser A, Holley-Guthrie E, Simpson D, Kaufmann W, Kenney S. The Epstein-Barr virus immediate-early protein BZLF1 induces both a G(2) and a mitotic block. J Virol 2002 Oct;76(19):10030–7. [PubMed: 12208981]
23. Kanda S, Mochizuki Y, Kanetake H. Stromal cell-derived factor-1alpha induces tube-like structure formation of endothelial cells through phosphoinositide 3-kinase. J Biol Chem 2003 Jan 3;278(1): 257–62. [PubMed: 12414810]
24. Oshima Y, Sato K, Tashiro F, Miyazaki J, Nishida K, Hiraki Y, et al. Anti-angiogenic action of the C-terminal domain of tenomodulin that shares homology with chondromodulin-I. J Cell Sci 2004 Jun 1;117(Pt 13):2731–44. [PubMed: 15150318]
25. Kozak M. Evaluation of the “scanning model” for initiation of protein synthesis in eucaryotes. Cell 1980 Nov;22(1 Pt 1):7–8. [PubMed: 7000367]
26. Liu L, Shao G, Steele-Perkins G, Huang S. The retinoblastoma interacting zinc finger gene RIZ produces a PR domain-lacking product through an internal promoter. J Biol Chem 1997 Jan 31;272 (5):2984–91. [PubMed: 9006946]
27. Gyory I, Fejer G, Ghosh N, Seto E, Wright KL. Identification of a functionally impaired positive regulatory domain I binding factor 1 transcription repressor in myeloma cell lines. J Immunol 2003 Mar 15;170(6):3125–33. [PubMed: 12626569]
28. Nishikata I, Sasaki H, Iga M, Tateno Y, Imayoshi S, Asou N, et al. A novel EVI1 gene family, MEL1, lacking a PR domain (MEL1S) is expressed mainly in t(1;3)(p36;q21)-positive AML and blocks G-CSF-induced myeloid differentiation. Blood 2003 Nov 1;102(9):3323–32. [PubMed: 12816872]
29. Gyory I, Wu J, Fejer G, Seto E, Wright KL. PRDI-BF1 recruits the histone H3 methyltransferase G9a in transcriptional silencing. Nat Immunol 2004 Mar;5(3):299–308. [PubMed: 14985713]
30. Feng Q, Wang H, Ng HH, Erdjument-Bromage H, Tempst P, Struhl K, et al. Methylation of H3-lysine 79 is mediated by a new family of HMTases without a SET domain. Curr Biol 2002 Jun 25;12(12): 1052–8. [PubMed: 12123582]
31. Coffin JD, Poole TJ. Endothelial cell origin and migration in embryonic heart and cranial blood vessel development. Anat Rec 1991 Nov;231(3):383–95. [PubMed: 1763820]
32. Nishikawa SI, Nishikawa S, Kawamoto H, Yoshida H, Kizumoto M, Kataoka H, et al. In vitro generation of lymphohematopoietic cells from endothelial cells purified from murine embryos. Immunity 1998 Jun;8(6):761–9. [PubMed: 9655490]
33. Sanchez M, Gottgens B, Sinclair AM, Stanley M, Begley CG, Hunter S, et al. An SCL 3′ enhancer targets developing endothelium together with embryonic and adult haematopoietic progenitors. Development 1999 Sep;126(17):3891–904. [PubMed: 10433917]
34. Sugiyama D, Tsuji K. Definitive hematopoiesis from endothelial cells in the mouse embryo; a simple guide. Trends Cardiovasc Med 2006 Feb;16(2):45–9. [PubMed: 16473761]
35. Downs KM, Harmann C. Developmental potency of the murine allantois. Development 1997 Jul;124 (14):2769–80. [PubMed: 9226448]
36. Caprioli A, Minko K, Drevon C, Eichmann A, Dieterlen-Lievre F, Jaffredo T. Hemangioblast commitment in the avian allantois: cellular and molecular aspects. Dev Biol 2001 Oct 1;238(1):64–78. [PubMed: 11783994]

37. Bollerot K, Pouget C, Jaffredo T. The embryonic origins of hematopoietic stem cells: a tale of hemangioblast and hemogenic endothelium. Apmis 2005 Nov-Dec;113(11–12):790–803. [PubMed: 16480450]

38. Kim KC, Geng L, Huang S. Inactivation of a histone methyltransferase by mutations in human cancers. Cancer Res 2003 Nov 15;63(22):7619–23. [PubMed: 14633678]

39. Tachibana M, Sugimoto K, Fukushima T, Shinkai Y. Set domain-containing protein, G9a, is a novel lysine-preferring mammalian histone methyltransferase with hyperactivity and specific selectivity to lysines 9 and 27 of histone H3. J Biol Chem 2001 Jul 6;276(27):25309–17. [PubMed: 11316813]

40. He L, Yu JX, Liu L, Buyse IM, Wang MS, Yang QC, et al. RIZ1, but not the alternative RIZ2 product of the same gene, is underexpressed in breast cancer, and forced RIZ1 expression causes G2-M cell cycle arrest and/or apoptosis. Cancer Res 1998 Oct 1;58(19):4238–44. [PubMed: 9766644]

41. Deng Q, Huang S. PRDM5 is silenced in human cancers and has growth suppressive activities. Oncogene 2004 Jun 17;23(28):4903–10. [PubMed: 15077163]

42. Lin Y, Wong K, Calame K. Repression of c-myc transcription by Blimp-1, an inducer of terminal B cell differentiation. Science 1997 Apr 25;276(5312):596–9. [PubMed: 9110979]

43. Shapiro-Shelef M, Lin KI, McHeyzer-Williams LJ, Liao J, McHeyzer-Williams MG, Calame K. Blimp-1 is required for the formation of immunoglobulin secreting plasma cells and pre-plasma memory B cells. Immunity 2003 Oct;19(4):607–20. [PubMed: 14563324]

44. Gupta S, Anthony A, Pernis AB. Stage-specific modulation of IFN-regulatory factor 4 function by Kruppel-type zinc finger proteins. J Immunol 2001 May 15;166(10):6104–11. [PubMed: 11342629]

45. Ghosh N, Gyory I, Wright G, Wood J, Wright KL. Positive regulatory domain I binding factor 1 silences class II transactivator expression in multiple myeloma cells. J Biol Chem 2001 May 4;276 (18):15264–8. [PubMed: 11279146]

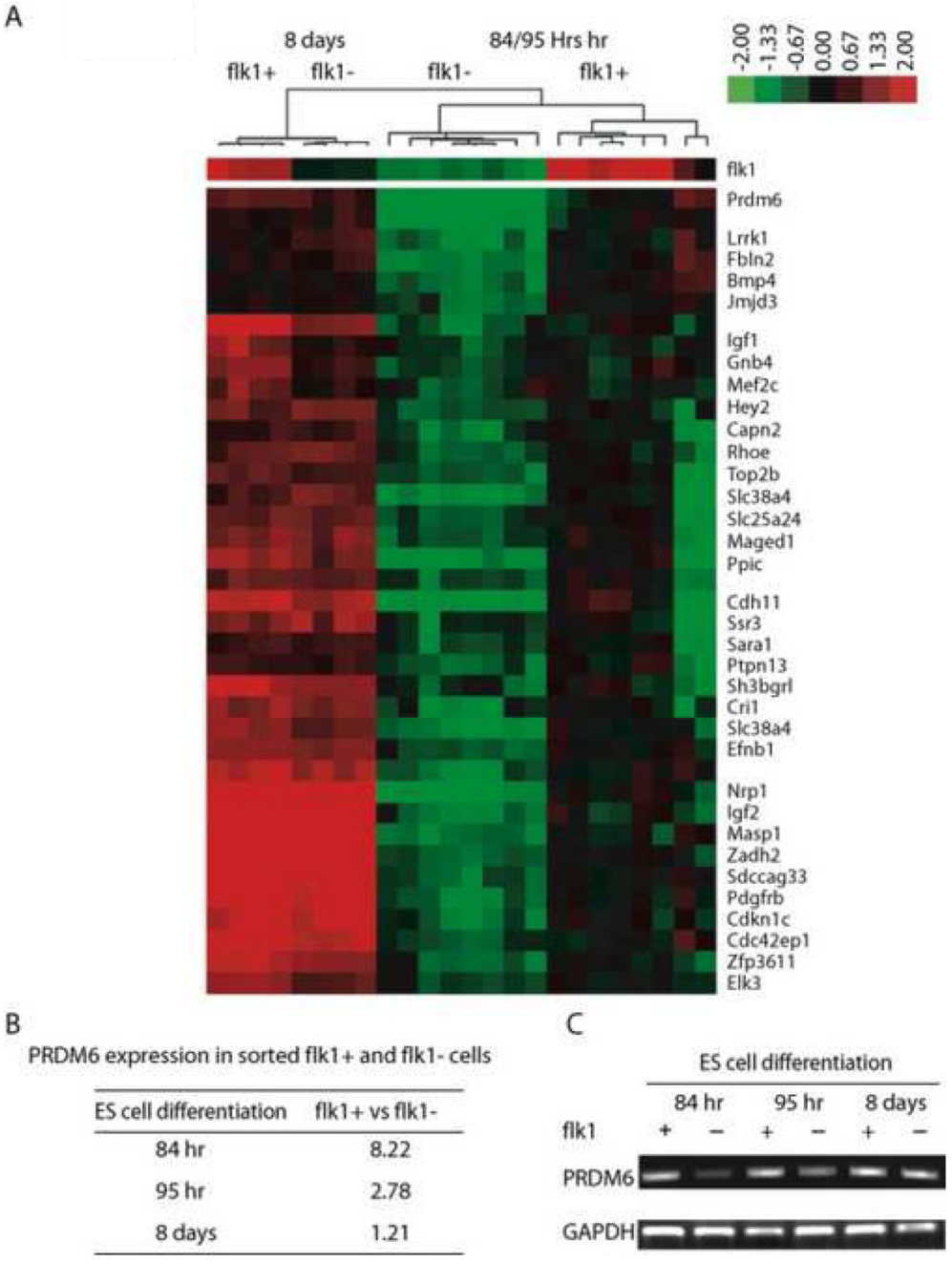

Figure 1. PRDM6 gene expression is enriched in flk1(+) vascular precursors

A. A hierarchical cluster was assembled from a previous microarray analysis [7] containing PRDM6 and co-expressed genes in flk1(+) and flk1(−) cells during ES cell differentiation. The color scale ranges from green for log ratio −2 to red for log ration +2, as indicated. *B.* Relative enrichment of PRDM6 mRNA in the flk1(+) cell population by microarray assay. *C.* Differential expression of PRDM6 mRNA was confirmed by RT-PCR.

A

B

```
MLKPGDPGGSAFLKVDPAYLQHWQQLFPPPPPERAEPPPDGLRPRPASLS  50
STPAPSSTSASSASSCAAAAAAAALAGLSALPVAQMPVFAPLAAAAVAAE 100
PLPPKDLCLGASAGPGPAKCGGGGGSVGDGRGVPRFRCSAEELDYYLYGQ 150
QRMEIIPLNQHTSDPNNRCDMCADNRNGECPMHGPLHSLRRLVGTSSAAA 200
AAPPPELPEWLRDLPREVCLCTSTVPGLAYGICAAQRIQQGTWIGPFQGV 250
LLSPEKVQTGVVRNTQHLWEIYDQDGTLQHFIDGGEPSKSSWMRYIRCAR 300
HCGEQNLTVVQYRSNIFYRACIDIPRGTELLVWYNDSYTSFFGIPLQCIA 350
QDENLNVPSTVMEAMCRQDALQPFNKSSKLSPSGQQRSVVFPQTPCSRNF 400
SLLDKSGPMEAGFNQINVKNQRVLASPTSTSQLHSEFSDWHLWKCGQCFK 450
TFTQRILLQMHVCTQNPDRPYQCGHCSQSFSQPSELRNHVVTHSSDRPFK 500
CGYCGRAFAGATTLNNHIRTHTGEKPFKCERCERSFTQATQLSRHQRMPN 550
ECKPITESPESIEVD*                                    565
```

C

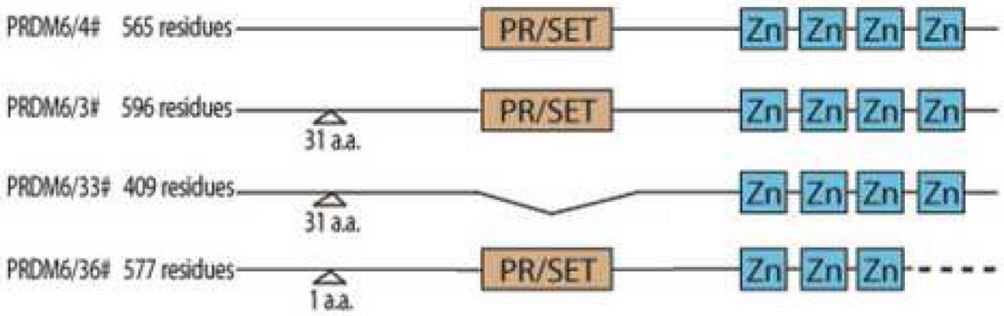

Figure 2. PRDM6 structure

A. Schematic map of mouse PRDM6/4# (isoform 4 of PRDM6) protein structure. The PR domain is shown in *brown* and the Krüpple-like zinc fingers (ZN) are shown in *blue*. The amino acid positions of the initiation codon and motifs are indicated. *B.* Deduced amino acid sequence of PRDM6/4#. *C*. Schematics of different PRDM6 isoforms cloned. Compared to PRDM6/4#, isoforms PRDM6/3#, PRDM6/33# and PRDM6/36# have additions of 31 a.a, 31 a.a and 1 a.a inserted after residue 28. PRDM6/33# also has a 187 a.a deletion including the entire PR domain. PRDM6/36# has different splicing between the third and forth ZN, resulting in loss of the fourth ZN, producing an alternative 48 residues at the carboxyl terminus. Insertion (Δ), deletion (∨) or alternative splicing (---) are marked compared to PRDM6/4#.

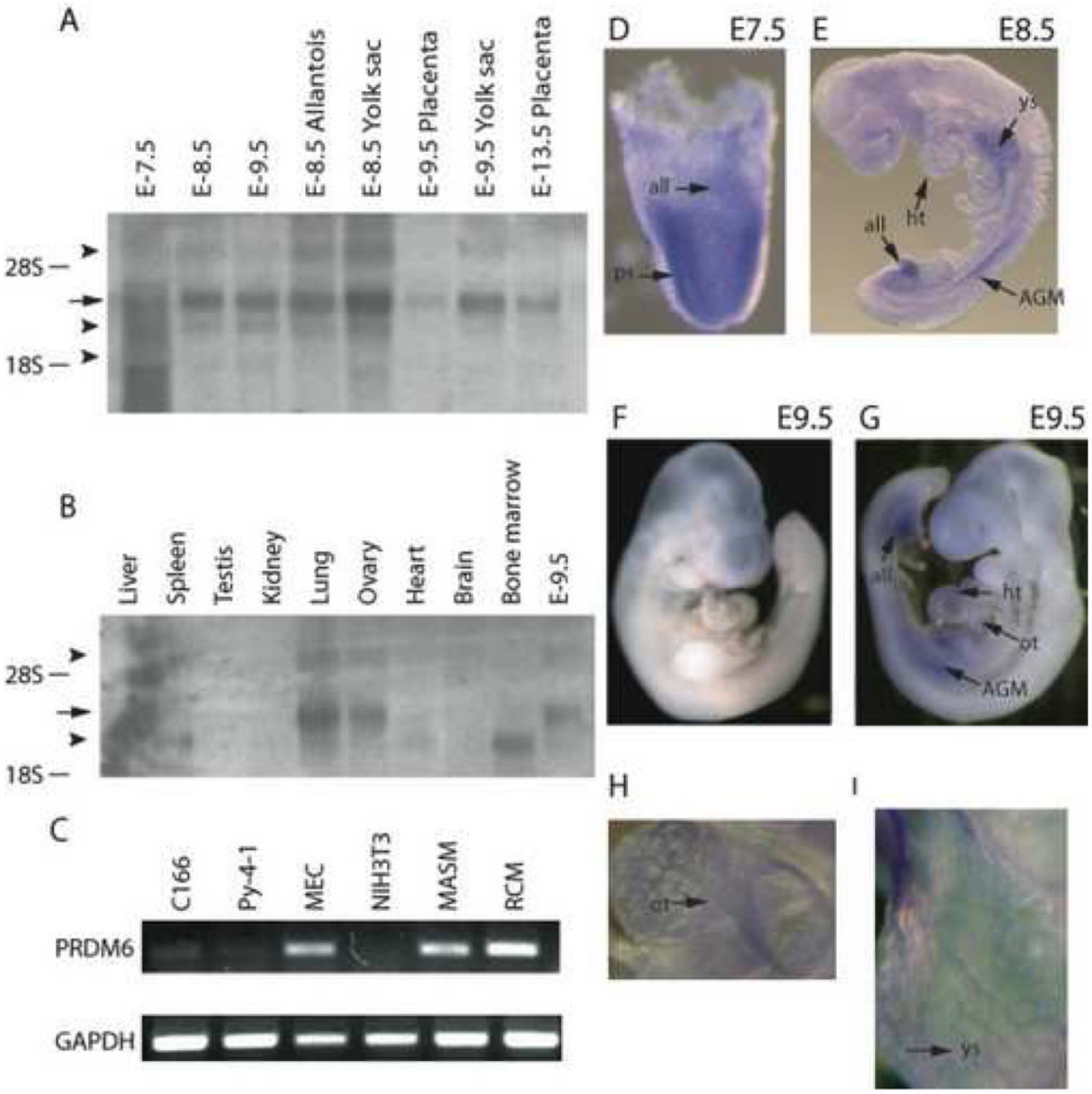

Figure 3. Tissue and cell distribution of PRDM6

A and B Total RNA from mouse embryos (*A*) and mouse adult tissues (*B*) were isolated. Northern blots were hybridized with a PRDM6 probe. One major (marked as *arrow*) and three minor (marked as *arrowhead*) types of PRDM6 were detected. *C*. Specific primers for PRDM6 were used to detect gene expression in different cell lines by RT-PCR. PRDM6 was detected in mouse endothelial cells MEC and C166, MASM and RCM. *D–I.* PRDM6 expression in early embryos. *D.* Specific staining with antisense probe was detected in the allantois and primitive streak regions. *E, G.* Detection of PRDM6 mRNA in the heart, outflow tract, and P-Sp/AGM region. *H.* Enlarged view of outflow tract from *G. I.* PRDM6 mRNA was detected in the vessels of E9.5 yolk sac. *F.* Control staining using sense probe. Abbreviations: all,

allantois; ps, primitive streak; ht, heart; ot, outflow tract; P-Sp/AGM, para-aortic splanchnopleura/aorta-gonad-mesonephros; ys, yolk sac.

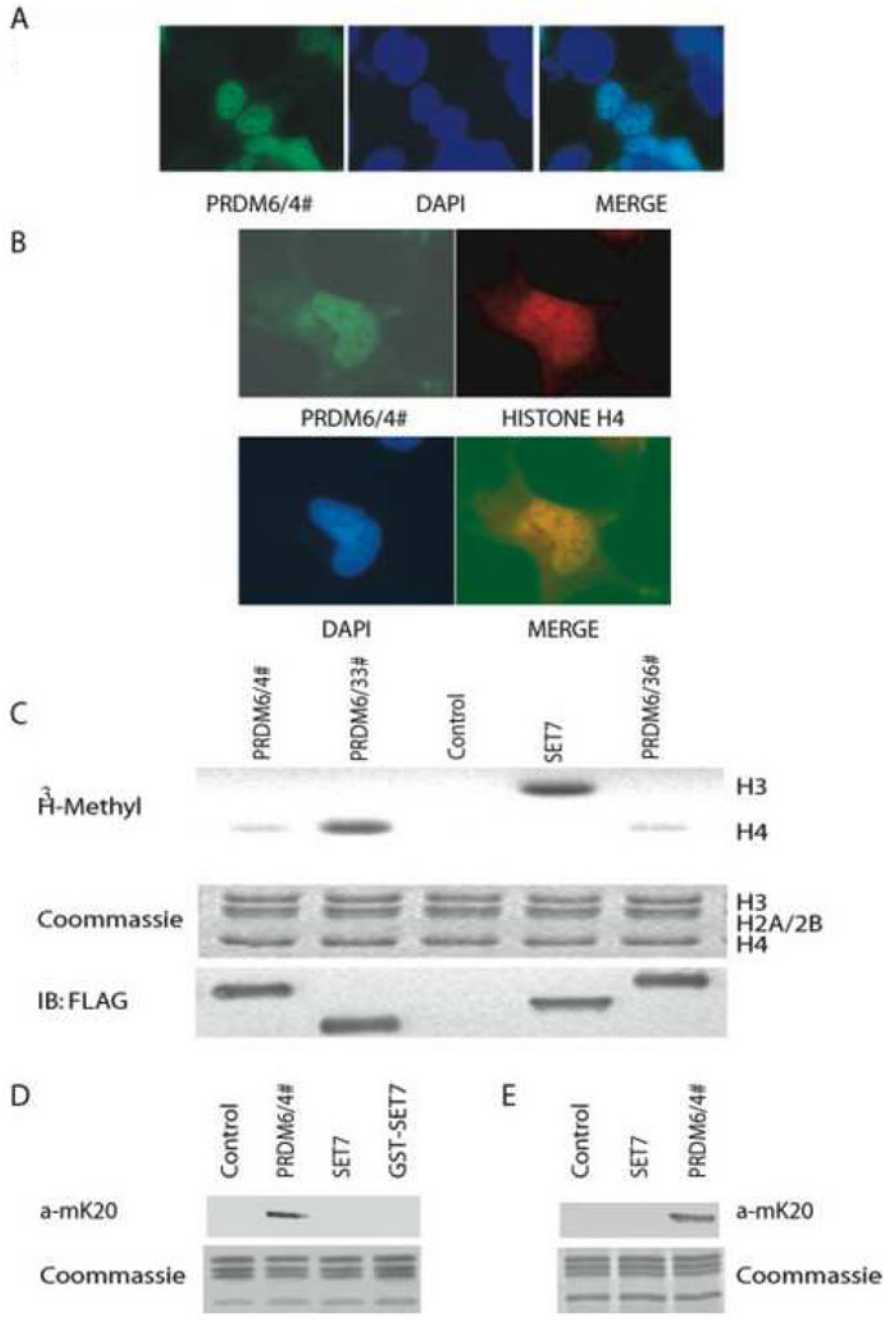

Figure 4. Nuclear localization and HMTase activity of PRDM6

A. FLAG-tagged plasmid pPRDM6/4# was transfected into HEK293 cells. After fixation, cells were immunostained with anti-FLAG antibody and DAPI and visualized by fluorescence microscopy. Magnifications 20X. *B.* PRDM6/4# co-localized with histone H4 in nucleus by confocal immunostaining assay. *C.* PRDM6/4# was immunoprecipitated by anti-FLAG antibody before enzymatic methyltransferase activity was measured. The amount of purified protein used in the assay was normalized by immunoblotting with anti-FLAG (lower panel). SET7 is used as a positive control. Samples derived from empty-vector transfected cells were used to control for nonspecific background. Methylated histones were visualized by SDS-PAGE and autoradiography (upper panel). The position of each histone substrate and the

amounts present in each assay is demonstrated by Coomassie blue staining of gel (middle panel). These results are representative of three independent experiments. *D*. HeLa cells were transfected with the indicated plasmids. HMTase assays were performed as for *C* except unlabeled SAM was used. Reaction mixtures were resolved by SDS-PAGE and methylation sites were determined by Western blotting analysis with specific antibodies. GST-SET7 was used as control for H3-K4 methylation. *E*. Core histones were extracted from transfected HeLa cells as indicated and electrophoresed by SDS-PAGE. *In vivo* methylation sites were detected by Western blotting analysis with specific antibodies.

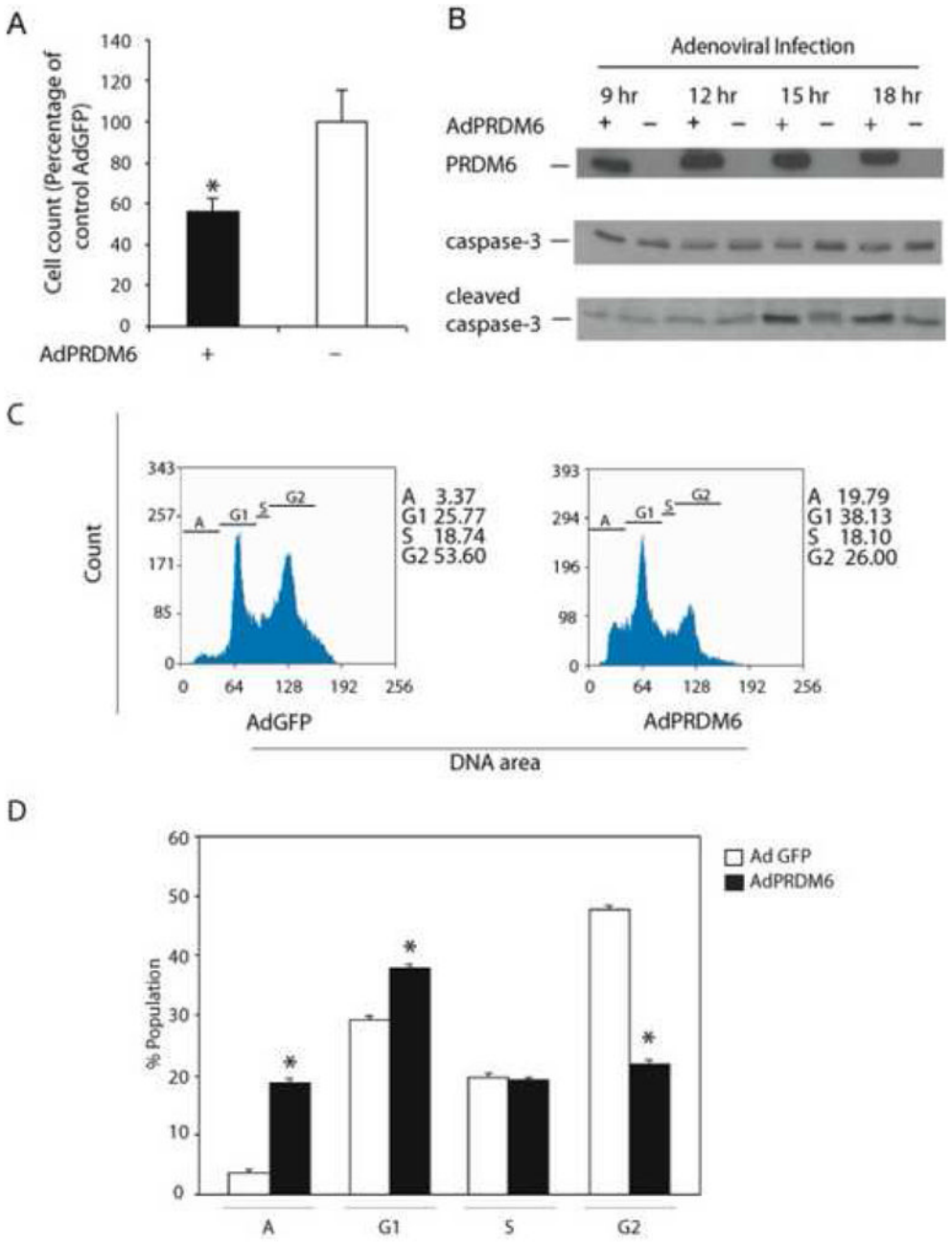

Figure 5. PRDM6-induced apoptosis and cell cycle arrest in MEC

A. Cell death was observed in MEC infected with AdPRDM6. Living cells were counted by trypan blue exclusion at 24 h post-infection. Shown is a representative of three independent experiments. Cell counts were expressed as a percentage of control cells with AdGFP infection. *B.* Western blot analysis of cell extracts from AdPRDM6-infected MEC. MEC cells were infected with AdPRDM6 or AdGFP. Cell lysates were harvested at various times post infection as indicated on top of each lane and were analyzed by immunoblot analysis using FLAG antibody (upper panel), caspase-3 antibody (middle panel) and cleaved caspase-3 antibody (lower panel). *C.* Cell cycle profile of MEC infected by AdPRDM6. Infected cells were analyzed by propidium iodide staining followed by flow cytometry. The percentages of cells that fall within the indicated gate are noted. Values of less than 2% represent background

staining. The Y-axis represents the relative cell number. The X-axis represents DNA content. A representative of four independent experiments is shown *D*. The results in *C* are expressed as the mean ± SD of three independent experiments. *, $P<0.01$.

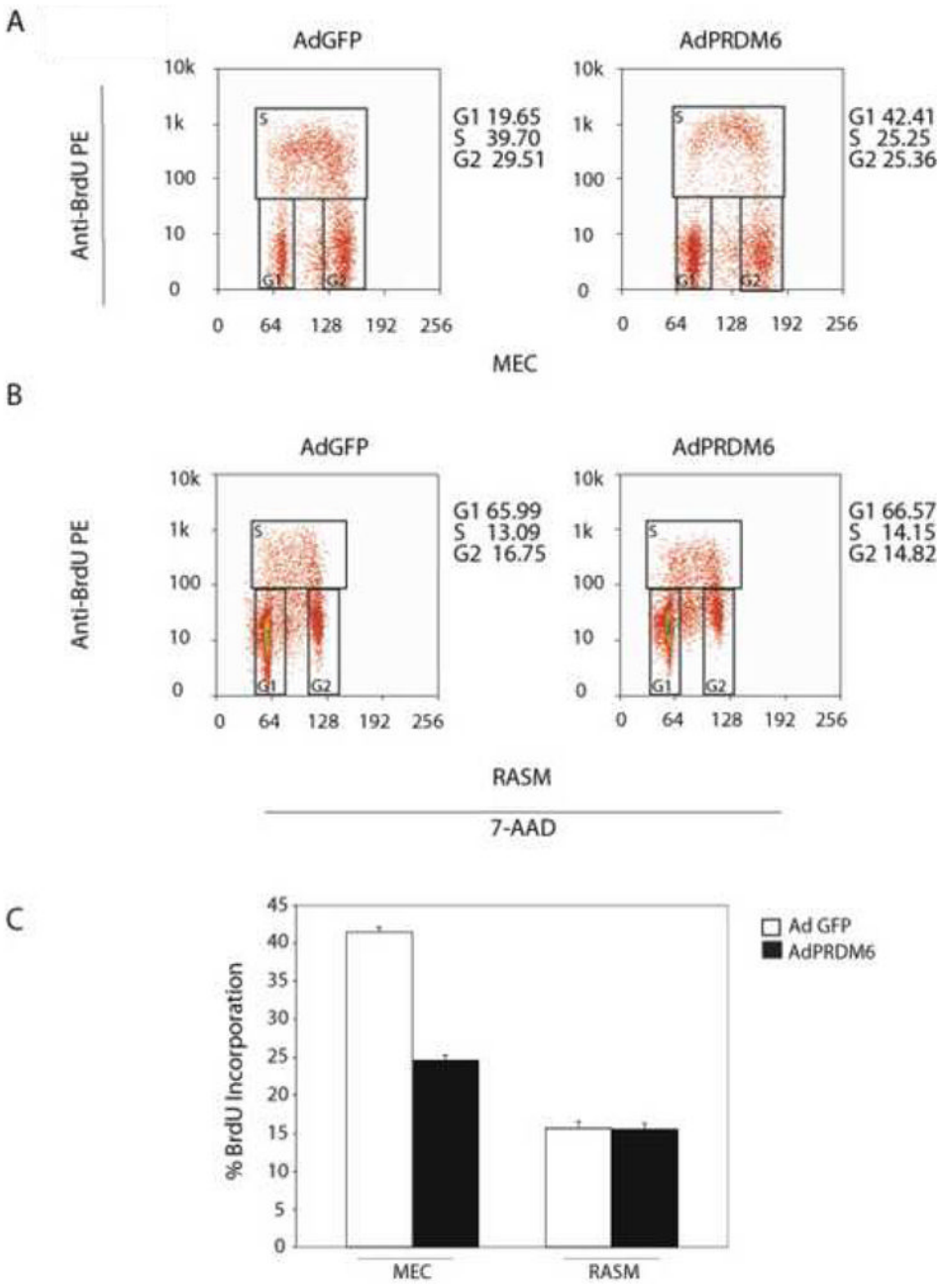

Figure 6. PRDM6 affects DNA synthesis in cell type-dependant manner

MEC (*A*) and RASM (*B*) were infected for 18 h and then were incubated with BrdU. BrdU incorporation was measured by flow cytometry after staining with anti-Brdu antibody and 7-AAD. The percentages of cells that fall within the indicated gate are noted. The Y-axis represents fluorescence intensity of BrdU-PE. The X-axis represents DNA content. *C.* Shown is representative experiment of three independent experiments in *A* and *B.*

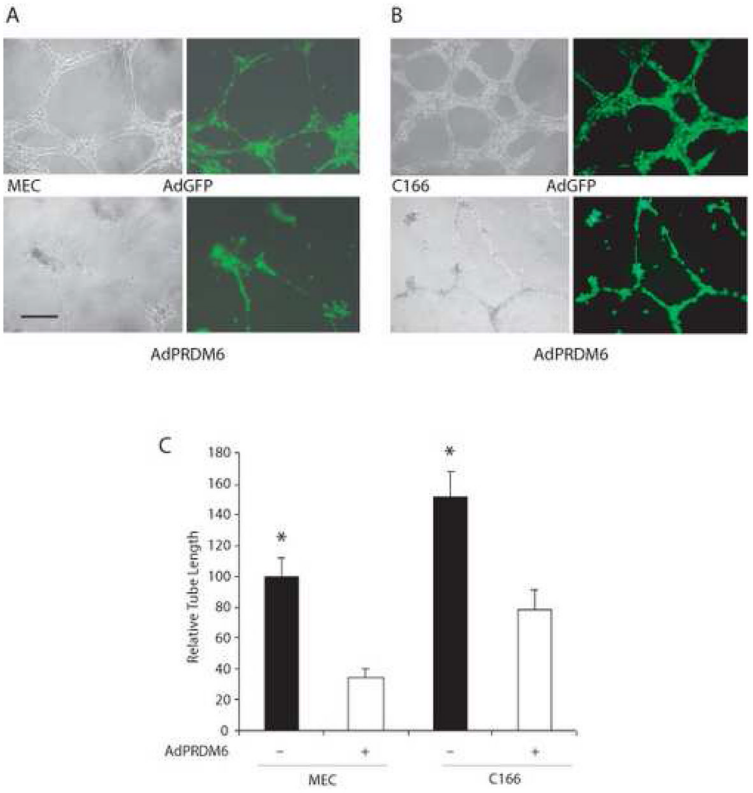

Figure 7. Effects of PRDM6 on endothelial cell assembly in Matrigel

MEC and C166 were infected with AdPRDM6 or AdGFP for 9 hr. Then equal numbers of cells were seeded onto growth factor-reduced Matrigel for 12 hr. Markedly decreased tube formation was observed in the AdPRDM6-infected cells. Representative micrographs show the capillary-like structures formed by MEC (*A*) and C166 (*B*). *Bar*, 100 μm. C. The results in *A* and *B* are expressed as the mean ± SD of three independent experiments. Tube length obtained from AdGFP-infected MEC was set to 100.*, $P<0.01$.